ISSN 1063-7834, Physics of the Solid State, 2014, Vol. 56, No. 8, pp. 1542–1547. © Pleiades Publishing, Ltd., 2014.
Original Russian Text © D.A. Balaev, S.I. Popkov, K.A. Shaikhutdinov, M.I. Petrov, D.M. Gokhfeld, 2014, published in Fizika Tverdogo Tela, 2014, Vol. 56, No. 8, pp. 1492–1497.

SUPERCONDUCTIVITY

Magnetoresistance of Porous Polycrystalline HTSC: Effect of the Transport Current on Magnetic Flux Compression in Intergranular Medium

D. A. Balaev[a, b, *], S. I. Popkov[a, b], K. A. Shaikhutdinov[a, b], M. I. Petrov[a], and D. M. Gokhfeld[a]

[a] *Kirensky Institute of Physics, Siberian Branch of the Russian Academy of Sciences, Akademgorodok 50–38, Krasnoyarsk, 660036 Russia*

* *e-mail: dabalaev@iph.krasn.ru*

[b] *Institute of Engineering Physics and Radio Electronics, Siberian Federal University, ul. Kirenskogo 28, Krasnoyarsk, 660074 Russia*

Received February 7, 2014

Abstract—The hysteretic dependences of the magnetoresistance of porous (38% of the theoretical density) granular high-temperature superconductor (HTSC) $Bi_{1.8}Pb_{0.3}Sr_{1.9}Ca_2Cu_3O_x$ have been analyzed in the model of the effective intergranular field. This effective field has been defined by the superposition of the external field and the field induced by magnetic moments of superconducting grains. The magnetic flux compression in an intergranular medium, characterized by the effective field, controls the hysteretic behavior of the magnetoresistance. It has been found that the magnetoresistance hysteresis width for the studied porous HTSC depends on the transport current, in contrast to the superconductor of the same composition with high physical density (more than 90% of the theoretical value). For a porous superconductor, a significant current concentration occurs in the region of the grain boundaries, which is caused by features of its microstructure. A current-induced increase in the effective boundary length results in a decrease in the flux compression, a decrease in the effective field in the intergranular medium, and a magnetoresistance hysteresis narrowing with increasing current.

DOI: 10.1134/S1063783414080034

1. INTRODUCTION

In the type-II granular superconductors placed in an external magnetic field, the magnetic flux distribution is extremely inhomogeneous in space. The magnetic field is weakened in superconducting grains and is concentrated in the grain boundary region. If the superconductor coherence length is comparable to the grain boundary length, which is valid for high-temperature superconductors (HTSCs), such a boundary behaves as a Josephson junction. For Josephson junctions of any type [1], the current–voltage (I–V) characteristic significantly changes under a magnetic field. Therefore, the significant magnetoresistance effect is observed in granular HTSCs, which is caused by dissipation processes in grain boundaries [2–23]. Detailed studies of the hysteretic dependences of the magnetoresistance $R(H)$ for yttrium [24, 25], bismuth [25], and lanthanum [25] HTSC systems showed that these characteristics are related to the magnetic flux compression in the grain boundary region [26, 27]. Due to the magnetic interaction of superconducting grains with field in the grain boundary region, the magnetic flux is compressed, and the magnetic induction can significantly exceed the external field [26–28].

In [24, 25], the model was proposed, which considers the effective field taking identical for the entire intergranular medium and proportional to the magnetic moment of superconductor grains. This model made it possible to explain main features of hysteretic dependences of the magnetoresistance of granular superconductors [20–30].

In this study, magnetoresistive properties of the low-density bismuth HTSC are analyzed within the mentioned approach. The low density (20–40% of the theoretical value [30–35]) in this material results from a large number of pores, and randomly spatially oriented Bi2223 grains are shaped as plates with large enough linear sizes and small thickness. In this case, grain cleavage regions are grain boundaries [32, 34, 35]. The sample magnetoresistance is controlled by these grain boundaries and carries information on the magnetic flux compression. This work is devoted the study of the magnetic flux concentration effect in grain boundaries of porous HTSC in an external magnetic field when transport current is passed through the sample.

2. SAMPLE PREPARATION AND EXPERIMENTAL TECHNIQUE

The previously obtained and characterized [31, 36] porous HTSC samples of composition

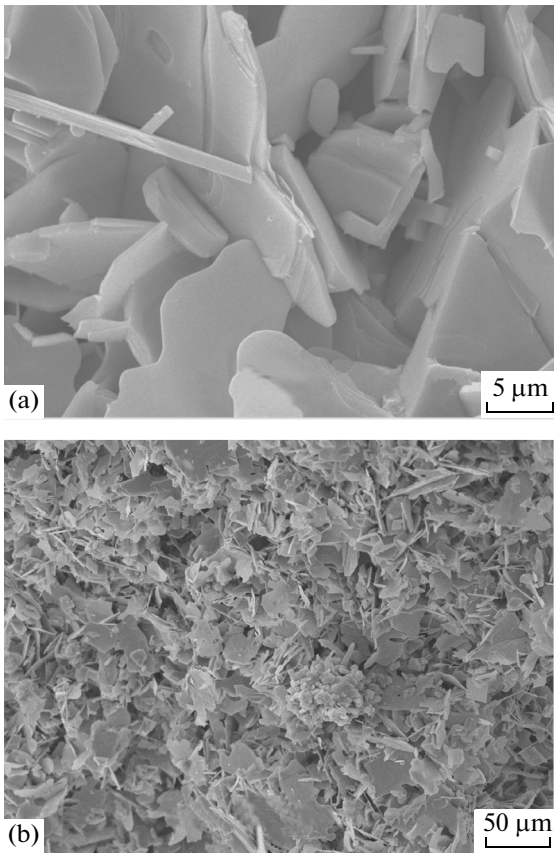

Fig. 1. Results of scanning electron microscopy for porous $Bi_{1.8}Pb_{0.3}Sr_{1.9}Ca_2Cu_3O_x$ with a bulk density of 2.26 g/cm^3.

$Bi_{1.8}Pb_{0.3}Sr_{1.9}Ca_2Cu_3O_x$ with a bulk density of 2.26 g/cm^3 (38% of the theoretical density) were studied. According to magnetic and electric measurements, the superconducting transition onset temperature is 108 K [31, 36].

The typical results of scanning electron microscopy (SEM) are shown in Fig. 1. The material consists of tabular grains with average in-plane sizes of ~10–20 μm and ~1 μm thick. It should be noted that, in this study, we make no distinction between the terms grain and crystallite. Grains touch each other only in small-area cleavage regions, so that there are numerous clearly distinguishable unfilled regions between grains (pores).

The magnetoresistance $R(H) = U(H)/I$, where U is the voltage drop and I is the transport current, was measured by the standard four-probe method in the constant current mode. The sample was shaped as a parallelepiped $1 \times 1.5 \times 9$ mm^3 in size. In the magnetoresistance measurements, the sample was in liquid nitrogen. The magnetization hysteresis loop $M(H)$ was measured using a vibrating magnetometer [37]. In magnetic and magnetoresistive measurements, the superconductor was cooled in zero external field; the

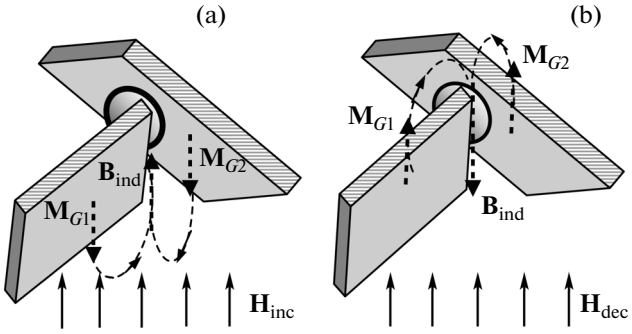

Fig. 2. Schematic representation of the relative orientation of the external field $\mathbf{H}$, grain magnetic moments $\mathbf{M}_{G1}$ and $\mathbf{M}_{G2}$, and the field B_{ind} induced by them in the grain boundary region for the studied porous HTSC (see Fig. 1). The grains are shown as plates. The plate contact region being a grain boundary is separated. The cases where the external field (a) increases ($H = H_{inc}$, $M_G < 0$) and (b) decreases ($H = H_{dec}$, $M_G > 0$) are shown.

dependences $R(H)$ and $M(H)$ were measured at a constant external field sweep rate (1 Oe/s). No special precautions on geomagnetic field shielding were undertaken.

3. MODEL

Let us consider the field distributions in the intergranular medium of granular HTSC. Since superconducting properties in grain boundaries are suppressed, an external field begins to penetrate initially into these regions upon reaching H_{C1J}. The latter quantity is called the first critical field for the Josephson medium [38]. For granular HTSCs, H_{C1J} as a rule does not exceed several oersteds at temperatures of the order of liquid nitrogen temperature [8, 9, 38].

In the range of fields higher than H_{C1J}, but lower than the first critical field of HTSC grains H_{C1}, the Meissner state is implemented in grains. The magnetic induction lines from the shielding supercurrent in superconducting grains are closed through grain boundaries. At $H > H_{C1}$, the external field partially penetrates grains; however, the situation does not change in principle, since the magnetic response of the type-II superconductor is a superposition of contributions of Meissner currents (diamagnetic response) and Abrikosov vortices (their magnetic moment is directed in parallel to the external field). Under different experimental conditions (an increase or decrease in the external field), the ratio of these contributions can vary, which appears in the magnetization hysteresis loop shape. The experimental hysteretic dependence $M(H)$ which reflects the above contributions can be used in the further analysis.

Figure 2 qualitatively illustrates the discussed pattern of magnetic induction lines the intergranular medium for the porous superconductor. The cases

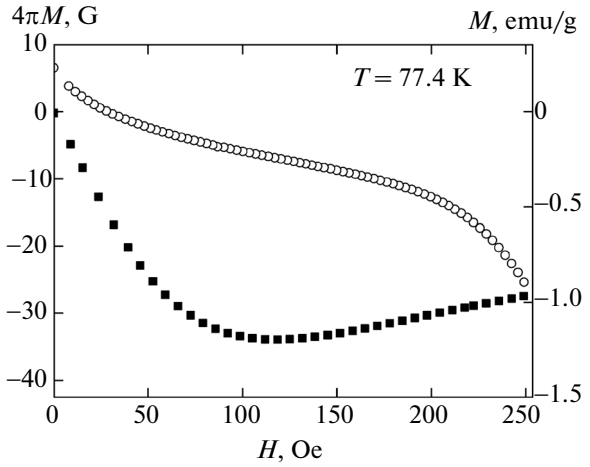

Fig. 3. Portion of the $M(H)$ hysteresis loop of the porous HTSC under study at $T = 77.4$ K. Closed and open symbols correspond to increasing ($H = H_{inc}$) and decreasing ($H = H_{dec}$) fields, respectively.

where $dH/dt > 0$ and $M(H) < 0$ (the external field increases and the HTSC magnetic moment is negative, see Fig. 3) and $dH/dt < 0$ ($M(H) > 0$) are shown. The magnetic flux in the grain boundary (grain cleavage region) is extremely sensitive to orientation of grains due to their anisotropy [39–42] (the c crystallographic axis is perpendicular to the grain plane); even for two adjacent grains, the calculation of the magnetic induction distribution is rather complicated.

In the case of a granular superconductor with random orientation of superconducting grains and grain boundaries, it is convenient to consider the effective field in the intergranular medium. To this end, the following simplifications should be made: (i) the effective field is identical in magnitude for all grain boundaries; (ii) the dependence $M(H)$ of the sample is similar to the dependence $M(H)$ of individual grains; (iii) the field B_{ind} induced by superconducting grains in the intergranular medium is proportional to the sample magnetic moment: $B_{ind}(H) = \pm\alpha \times 4\pi M(H)$, where the parameter α includes averaging over grain demagnetizing factors and defines the compression ratio of the magnetic flux in the intergranular medium (grain cleavage region). Then, the effective field B_{eff} in the intergranular medium is given by the expression

$$B_{eff}(H) = H - \alpha \times 4\pi M(H), \qquad (1)$$

in which the relative directions of the vectors $\mathbf{M}$, B_{ind}, and B_{eff} sign are taken into account. At $H > 0$ and $dH/dt > 0$, $M < 0$ and the induced field $B_{ind} > 0$ (locally, $B_{ind} \parallel \mathbf{H}$, see Fig. 2a); in this case, $B_{eff} > 0$. On the contrary, at $H > 0$ and $dH/dt < 0$, $M > 0$ and $B_{ind} < 0$ (locally, $\mathbf{B}_{ind}$ is antiparallel to $\mathbf{H}$, see Fig. 2b). In the latter case, in the region of relatively weak fields, B_{ind} can exceed H, and B_{eff} will change sign. The magnetoresistance $R(H)$ caused by dissipation processes in grain boundaries is defined by the effective field in the intergranular medium; since the B_{eff} sign is not important for these processes, R is a certain function of the B_{eff} magnitude, i.e., $R(H) = f(|B_{eff}(H)|)$.

Since the dependence $M(H)$ is hysteretic (due to vortex pinning within grains), the dependences $B_{eff}(H)$, hence, $R(H)$ are also hysteretic. As shown in [22, 26, 27], an analysis of the dependences $|B_{eff}(H)|$ obtained from experimental data on the magnetization $M(H)$ allows us to explain the main features of the hysteretic dependences of the magnetoresistance $R(H)$.

Due to the I–V characteristic nonlinearity, the magnetoresistance depends also on the transport current. Therefore, to analyze the hysteretic dependences $R(H)$, it was proposed to consider the current-independent parameter, i.e., the field width ΔH of the magnetoresistance hysteresis [24, 25]. The field dependence of ΔH is given by $\Delta H(H_{dec}) = H_{dec} - H_{inc}$, where H_{inc} and H_{dec} are the increasing ($dH/dt > 0$) and decreasing ($dH/dt < 0$) fields for which the equalities $R(H_{inc}) = R(H_{dec})$ are satisfied, hence, $|B_{eff}(H_{inc})| = |B_{eff}(H_{dec})|$. Using expression (1), we obtain

$$\Delta H(H_{dec}) = \alpha \times 4\pi(M(H_{inc}) - M(H_{dec})). \qquad (2)$$

The parameter ΔH for most studied systems (yttrium [24, 25], lanthanum, and bismuth [25–27, 29] granular HTSCs) is independent of the transport current at which the magnetoresistance was measured. For the yttrium and bismuth systems, the intragranular critical current density is typically 10^4–10^5 A/cm^2 in the region of liquid-nitrogen temperatures. It is 2–3 orders of magnitude higher than transport current densities which can be achieved for granular bulk samples without an appreciable heating effect. However, the effect of the transport current on Abrikosov vortices within grains (pinned vortex separation, flux creep, and others) would be experimentally detectable if the transport current density is of the order of the critical current density in superconducting grains. Thus, the transport current did not change magnetic properties of HTSC grains (dependences $M(H_{inc})$ and $M(H_{dec})$) in [24, 25]. The dependence $\Delta H(H)$ was also unchanged at different currents I. The fact under consideration gave grounds to argue that the magnetic flux pinning is absent in the region of grain boundaries at $T = 77$ K. Otherwise, a current increase would lead to a change in the mode from the flux creep to flux in an intergranular medium and, eventually, to the dependence of ΔH on I [24, 25, 29].

In [23], a decrease in the parameter ΔH was analyzed in the case where the dependence $R(H)$ is close to flattening and the $R(H)$ hysteresis becomes small, so that the effective-field approximation in the intergranular medium becomes invalid. In the model under consideration, it is assumed that the magnetoresis-

tance is controlled only by the intergranular medium, i.e., the contribution of HTSC grains to dissipation is absent for used external fields.

4. RESULTS AND DISCUSSION

The experimental hysteretic dependences of the magnetization $M(H)$ and $R(H)$, obtained under identical experimental conditions, are shown in Figs. 3 and 4a. The magnetoresistance was measured at transport currents I from 40 to 500 mA. The critical current in zero external field $I_C(H = 0)$ for this sample is ≈580 mA; therefore, the dependences $R(H)$ in Fig. 4a start from the origin of coordinates (at $H = 0$, $R = 0$). The behavior of the dependences $R(H)$ is qualitatively well explained within the considerations presented in the previous section. However, in contrast to the previous results for samples of yttrium, bismuth, and lanthanum systems, the effect of the transport current on the dependence $\Delta H(H)$ is observed. The horizontal segment in Fig. 4a show ΔH at $H_{dec} = 200$ Oe. As the transport current increases, ΔH in the field $H_{dec} = 200$ Oe appreciably decreases. Previously [25], it was found that ΔH is independent of the transport current for the sample of the same composition, but with a density of ≈90% of the theoretical), under similar experimental conditions (temperature, field and current ranges).

Let us consider possible causes of the decrease in the hysteresis field width with increasing transport current. The density of the intragranular critical current in zero external field for this porous sample, determined by the Bean model from the $M(H)$ data (Fig. 3), is 10^4 A/cm^2. We note that the use of the Bean model in weak fields results in underestimation of the critical current density. The density of the transport current through the sample varies within 2.7–33 A/cm^2; the same taking into account the presence of pores (the sample density is 38% from the theoretical) is 7–88 A/cm^2. Hence, the transport current density within grains is much lower than the critical one, and the current cannot affect the magnetic moment of grains. Thus, it can be considered that $M(H_{inc})$ and $M(H_{dec})$ remain unchanged. It follows from (2) that the change in ΔH through transport current variations can be associated only with a change in the parameter α.

The behavior of the magnetoresistance $R(H)$ is controlled by hysteretic dependences $B_{eff}(H)$ which can be obtained from $M(H)$ loops (Fig. 3). Figure 4b shows the dependences $B_{eff}(H)$ at different parameters α. When constructing these dependences, the values of α were selected, at which the values ΔH from the dependences $R(H)$ and $B_{eff}(H)$ coincide in the field range of 100–250 Oe (Fig. 5). The change in the parameter α from 15 to 7.5 reflects well the observed decrease in the hysteresis field width, obtained from the dependences $R(H)$, which is illustrated in Fig. 5.

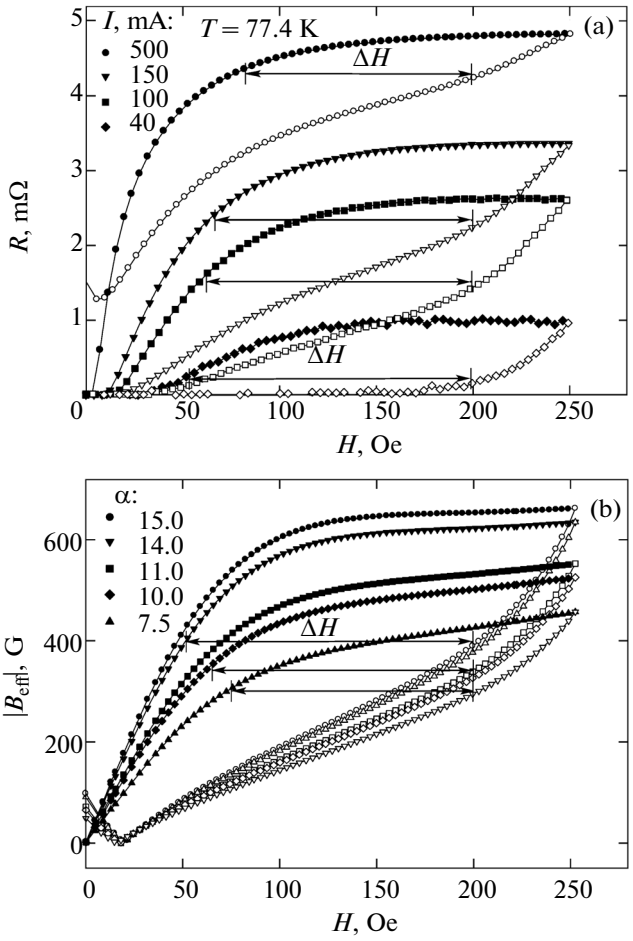

Fig. 4. (a) Hysteretic dependences of the magnetoresistance $R(H)$ at different transport currents I and (b) hysteretic dependences of the effective field magnitude $|B_{eff}(H)|$ in the intergranular medium, obtained from the data on $M(H)$ (Fig. 3) by formula (1) at different parameters α. Closed and open symbols correspond to increasing ($H = H_{inc}$) and decreasing ($H = H_{dec}$) fields, respectively. Horizontal segments show the hysteresis field width ΔH at $H_{dec} = 200$ Oe.

Granular HTSCs can be considered as a Josephson medium in which grain boundaries are barriers, i.e., "normal" regions separating superconducting banks. The effective size of the "normal region" L is defined by both the geometrical thickness of the grain boundary and superconducting grain parameters. As the transport current increases, L increases due to Joule heating and the corresponding decrease in the superconducting order parameter in the boundary regions of superconducting grains [43]. An increase in the effective thickness L of grain boundaries leads to an increase in the regions (non-superconducting or "normal") into which the magnetic field can freely penetrate, which should result in a decrease in the magnetic flux concentration effect. As the size of the grain boundary containing the magnetic flux increases, the local magnetic induction in it decreases. In the

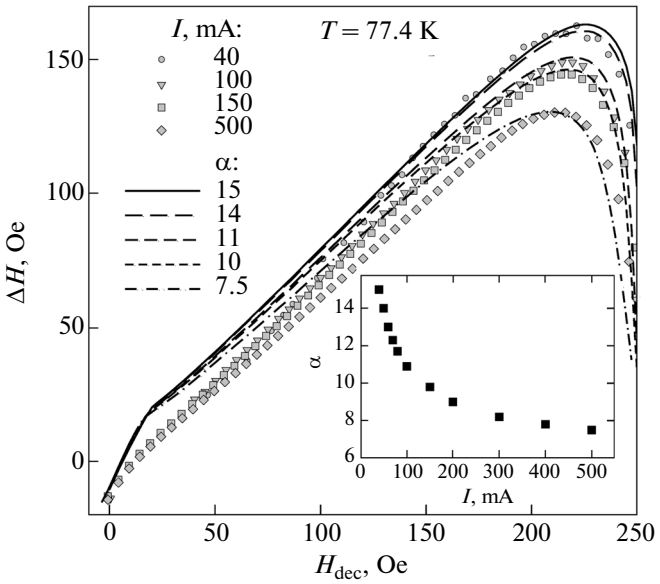

Fig. 5. Dependences of the hysteresis field width ΔH on the external field H_{dec}, obtained from the dependences $R(H)$ (Fig. 4a) (symbols) and from the dependences $|B_{eff}(H)|$ (Fig. 4b) (curves). The inset shows the dependence of the parameter α on the transport current I.

described scenario, the parameter α is proportional to L, and the experimentally observed decrease in the field width of the hysteresis with decreasing α is associated with an increase in "normal" regions. Thus, the dependence of α on I is associated with an increase in L with the current density. It can be concluded that α varied from 15 to 7.5 as the current was varied from 40 to 500 mA (Fig. 5); accordingly, the effective boundary thickness twofold increased.

Such an appreciable effect of I on L necessitates that the transport current density would be much more higher than the critical current density of weak link. For the previously studied samples with sufficiently high physical density, including bismuth HTSC, this condition was not satisfied under similar experimental conditions [25]. We can distinguish the following features characteristic of porous granular HTSC in comparison with dense samples: (i) the transport current in the porous sample flows over a smaller number of trajectories [44]; (ii) contact (cleavage) regions of grains in the porous sample have probably a smaller area than in the dense sample; (iii) the porous sample or even grain clusters not involved when current flows through the sample (dead ends). These features lead to that the current density through a typical grain boundary in the porous sample will be 1–2 orders of magnitude higher than in a dense granular sample at the same transport current. Therefore, in porous samples, the effect of the current on the hysteresis field width ΔH, related to the dependence of L on I is observed due to the current concentration in grain boundaries.

The effect of sizes and dimension of "normal" regions in superconductors on I–V characteristics during transport current flow was studied in the works by Kuzmin [45, 46]. For porous HTSCs, the dependence of the "normal region" sizes on the transport current and magnetic field was detected previously [35, 47].

5. CONCLUSIONS

It was found that the effect of magnetic flux compression in the intergranular medium of porous granular HTSC $Bi_{1.8}Pb_{0.3}Sr_{1.9}Ca_2Cu_3O_x$, which controls the hysteretic behavior of the magnetoresistance $R(H)$, depends on the transport current.

For porous HTSC, the field width ΔH of the magnetoresistance hysteresis significantly decreases with increasing transport current I, whereas ΔH of dense samples is independent of I under similar experimental conditions. The observed ΔH behavior was explained by the fact that the porous HTSC microstructure causes a significant current concentration in grain boundaries. Therefore, in the case of a comparatively low transport current, the geometrical extent of non-superconducting regions in grain boundaries of porous HTSC increases. The increase in the size of non-superconducting regions, into which the magnetic flux penetrates, results in the decrease in the effective field in the intergranular medium and the observed magnetoresistance hysteresis narrowing.

REFERENCES

1. A. Barone and G. Paterno, *Physics and Applications of the Josephson Effect* (Wiley, New York, 1982; Mir, Moscow, 1984).
2. M. A. Dubson, S. T. Herbert, J. J. Calabrese, D. C. Harris, B. R. Patton, and J. C. Garland, Phys. Rev. Lett. **60** (11), 1061 (1988).
3. C. Gaffney, H. Petersen, and R. Bednar, Phys. Rev. B: Condens. Matter **48** (5), 3388 (1993).
4. H. S. Gamchi, G. J. Russel, and K. N. R. Taylor, Phys. Rev. B: Condens. Matter **50** (17), 12950 (1994).
5. A. V. Mitin, Physica C (Amsterdam) **235–240**, 3311 (1994).
6. L. Urba, C. Acha, and V. Bekeris, Physica C (Amsterdam) **279**, 92 (1997).
7. A. C. Wright, K. Zhang, and A. Erbil, Phys. Rev. B: Condens. Matter **44** (2), 863 (1991).
8. N. D. Kuz'michev, JETP Lett. **74** (5), 262 (2001).
9. N. D. Kuz'michev, Phys. Solid State **43** (11), 2012 (2001).
10. D. A. Balaev, K. A. Shaihutdinov, S. I. Popkov, D. M. Gokhfeld, and M. I. Petrov, Supercond. Sci. Technol. **17**, 175 (2004).
11. D. A. Balaev, A. G. Prus, K. A. Shaykhutdinov, D. M. Gokhfeld, and M. I. Petrov, Supercond. Sci. Technol. **20**, 495 (2007).

12. V. V. Derevyanko, T. V. Sukhareva, and V. A. Finkel', Phys. Solid State **48** (8), 1455 (2006).
13. T. V. Sukhareva and V. A. Finkel', Phys. Solid State **50** (6), 1001 (2008).
14. T. V. Sukhareva and V. A. Finkel, J. Exp. Theor. Phys. **107** (5), 787 (2008).
15. T. V. Sukhareva and V.A. Finkel, Phys. Solid State **53** (5), 914 (2011).
16. V. V. Derevyanko, T. V. Sukhareva, and V. A. Finkel, Tech. Phys. **53** (3), 321 (2008).
17. V. V. Derevyanko, T. V. Sukhareva, and V. A. Finkel', Phys. Solid State **49** (10), 1829 (2007).
18. V. V. Derevyanko, T. V. Sukhareva, V. A. Finkel, and Yu. N. Shakhov, Phys. Solid State **56** (4), 649 (2014).
19. M. A. Vasyutin, Tech. Phys. Lett. **39** (12), 1078 (2013).
20. M. Olutas, A. Kilic, K. Kilic, and A. Altinkok, J. Supercond. Novel Magn. **26**, 3369 (2013).
21. A. Altinkok, K. Kilic, M. Olutas, and A. Kilic, J. Supercond. Novel Magn. **26**, 3085 (2013).
22. D. A. Balaev, A. A. Bykov, S. V. Semenov, S. I. Popkov, A. A. Dubrovskii, K. A. Shaikhutdinov, and M. I. Petrov, Phys. Solid State **53** (5), 922 (2011).
23. D. A. Balaev, A. A. Dubrovskii, S. I. Popkov, D. M. Gokhfeld, S. V. Semenov, K. A. Shaykhutdinov, and M. I. Petrov, Phys. Solid State **54** (11), 2155 (2012).
24. D. A. Balaev, D. M. Gokhfel'd, A. A. Dubrovskii, S. I. Popkov, K. A. Shaikhutdinov, and M. I. Petrov, J. Exp. Theor. Phys. **105** (6), 1174 (2007).
25. D. A. Balaev, A. A. Dubrovskii, K. A. Shaikhutdinov, S. I. Popkov, D. M. Gokhfeld, Yu. S. Gokhfeld, and M. I. Petrov, J. Exp. Theor. Phys. **108** (2), 241 (2009).
26. D. A. Balaev, S. I. Popkov, E. I. Sabitova, S. V. Semenov, K. A. Shaykhutdinov, A. V. Shabanov, and M. I. Petrov, J. Appl. Phys. **110**, 093918 (2011).
27. D. A. Balaev, S. V. Semenov, and M. I. Petrov, Phys. Solid State **55** (12), 2422 (2013).
28. D. Daghero, P. Mazzetti, A. Stepanesku, P. Tura, and A. Masoero, Phys. Rev. B: Condens. Matter **66**, 184514 (2002).
29. D. A. Balaev, A. A. Dubrovskii, S. I. Popkov, K. A. Shaikhutdinov, and M. I. Petrov, Phys. Solid State **50** (6), 1014 (2008).
30. K. A. Shaikhutdinov, D. A. Balaev, S. I. Popkov, and M. I. Petrov, Phys. Solid State **51** (6), 1105 (2009).
31. M. I. Petrov, T. N. Tetyueva, L. I. Kveglis, A. A. Efremov, G. M. Zeer, K. A. Shaikhutdinov, D. A. Balaev, S. I. Popkov, and S. G. Ovchinnikov, Tech. Phys. Lett. **29** (12), 986 (2003).
32. D. A. Balaev, I. L. Belozerova, D. M. Gokhfeld, L. V. Kashkina, Yu. I. Kuzmin, C. R. Michel, M. I. Petrov, S. I. Popkov, and K. A. Shaikhutdinov, Phys. Solid State **48** (2), 207 (2006).
33. D. M. Gokhfeld, D. A. Balaev, S. I. Popkov, K. A. Shaykhutdinov, and M. I. Petrov, Physica C (Amsterdam) **434**, 135 (2006).
34. K. A. Shaikhutdinov, D. A. Balaev, S. I. Popkov, and M. I. Petrov, Supercond. Sci. Technol. **20**, 491 (2007).
35. K. Yu. Terent'ev, D. M. Gokhfel'd, S. I. Popkov, K. A. Shaikhutdinov, and M. I. Petrov, Phys. Solid State **53** (12), 2409 (2011).
36. M. I. Petrov, D. A. Balaev, I. L. Belozerova, S. I. Popkov, A. A. Dubrovskii, K. A. Shaykhutdinov, and O. N. Mart'yanov, Tech. Phys. **54** (8), 1130 (2009).
37. A. D. Balaev, Yu. V. Boyarshinov, M. M. Karpenko, and B. P. Khrustalev, Prib. Tekh. Eksp., No. 3, 167 (1985).
38. E. B. Sonin, JETP Lett. **47** (8), 496 (1988).
39. G. C. Han, Phys. Rev. B: Condens. Matter **52**, 1309 (1995).
40. G. C. Han and C. K. Ong, Phys. Rev. B: Condens. Matter **56**, 11299 (1997).
41. D. C. van der Laan, J. Schwartz, B. ten Haken, M. Dhalle, and H. J. N. van Eck, Phys. Rev. B: Condens. Matter **77**, 104514 (2008).
42. D. A. Balaev, S. I. Popkov, S. I. Semenov, A. A. Bykov, K. A. Shaikhutdinov, D. M. Gokhfeld, and M. I. Petrov, Physica C (Amsterdam) **470**, 61 (2010).
43. D. Hazra, L. M. A. Pascal, H. Courtois, and A. K. Gupta, Phys. Rev. B: Condens. Matter **82**, 184530 (2010).
44. D. M. Gokhfeld, D. A. Balaev, K. A. Shaykhutdinov, S. I. Popkov, and M. I. Petrov, Physica C (Amsterdam) **467**, 80 (2007).
45. Yu. I. Kuzmin, Phys. Solid State **43** (7), 1199 (2001).
46. Yu. I. Kuzmin, Tech. Phys. Lett. **29** (5), 414 (2003).
47. M. A. Vasyutin, Tech. Phys. Lett. **37** (8), 743 (2011).

Translated by A. Kazantsev